Published in final edited form as:
Nat Cell Biol. 2016 April ; 18(4): 451–457. doi:10.1038/ncb3325.

Godzilla-dependent transcytosis promotes Wingless signalling in *Drosophila* wing imaginal discs

Yasuo Yamazaki[2,*], **Lucy Palmer**[1,*], **Cyrille Alexandre**[1], **Satoshi Kakugawa**[1], **Karen Beckett**[1], **Isabelle Gaugue**[3], **Ruth H. Palmer**[2,@], and **Jean-Paul Vincent**[1,@]

[1]The Francis Crick Institute, Mill Hill Laboratory, The Ridgeway, Mill Hill, London NW7 1AA, UK

[2]Dept. of Medical Biochemistry and Cell Biology, Institute of Biomedicine, The Sahlgrenska Academy at the University of Gothenburg, Medicinaregatan 9A, 40539 Gothenburg, SWEDEN

[3]Polarity, Division and Morphogenesis Team, Institut Curie, CNRS UMR 3215, INSERM U934, 26 rue d'Ulm, 75248 Paris Cedex 05, France

Abstract

The apical and basolateral membranes of epithelia are insulated from each other, preventing the transfer of extracellular proteins from one side to the other[1]. Thus, a signalling protein produced apically is not expected to reach basolateral receptors. Evidence suggests that Wingless, the main *Drosophila* Wnt is secreted apically in the embryonic epidermis[2, 3]. However, in the wing imaginal disc epithelium, Wingless is mostly seen on the basolateral membrane where it spreads from secreting to receiving cells [4, 5]. Here we examine the apico-basal movement of Wingless in Wingless-producing cells of wing imaginal discs. We find that it is presented first on the apical surface before making its way to the basolateral surface, where it is released and allowed to interact with signalling receptors. We show that Wingless transcytosis involves Dynamin-dependent endocytosis from the apical surface. Subsequent trafficking from early apical endosomes to the basolateral surface requires Godzilla, a member of the RNF family of membrane-anchored E3 ubiquitin ligases. Without such transport, Wingless signalling is strongly reduced in this tissue.

Keywords

Wnt; Transcytosis; Intracellular trafficking; Epithelia; Signalling; Ubiquitin ligase

Address correspondence to jp.vincent@crick.ac.uk or ruth.palmer@gu.se.

Author contributions

All the experiments with imaginal discs were performed by LP and YY. Genome engineering was performed by CA with help from IG. The project was conceived and elaborated by YY, LP, CA, RP, and JPV. The first draft of the paper was written by JPV with substantial subsequent contributions from RP, LP, YY, and CA. These authors also contributed to the design and interpretation of experiments.

[*]Equivalent first authors

[@]Equivalent senior authors

Europe PMC Funders Author Manuscripts

Two immunofluorescence staining protocols were used to examine the apico-basal distribution of Wingless in wing imaginal discs. The standard protocol, which includes a permeabilisation step, is expected to show intracellular and extracellular protein. Because of relatively higher abundance of Wingless in the intracellular pool, this method preferentially highlights intracellular Wingless. With this protocol, Wingless was seen to accumulate largely in the apical region (Fig. 1 a-d). Since *wingless* mRNA, as detected by fluorescence *in situ* hybridisation (FISH) (Fig. 1 e-h), also localises to the apical region, it is likely that intracellular Wingless protein accumulates there because this is where it is predominantly translated. To detect extracellular Wingless, imaginal discs were stained and fixed in the absence of detergent [4]. With this staining protocol, Wingless was seen mostly along the basolateral surface of producing and nearby receiving cells (Fig. 1 i-l). Although Wingless was enriched along the basal half, some signal could be detected up to the level of adherens junctions, as recognised with anti-E-Cadherin (Supplementary Fig. 1 a). Overall these observations suggest that Wingless protein is produced in the apical region and that somehow it is transported to the basolateral surface in order to be released in the extracellular space.

To confirm that Wingless is indeed first produced apically before proceeding to the basolateral surface, we devised a method to track it in the secretory pathway and beyond. Two *wingless* cDNAs, each carrying a different epitope tag were inserted in tandem at the *wingless* locus in such a way that no endogenous Wingless activity remained, and only the first cDNA (OLLAS-tagged) was expressed (Fig. 2 a). This first cDNA was flanked by Flp recombination targets (FRT sites, denoted as F in the genotypes below) allowing its excision upon Flp expression. Since excision also removes the transcriptional termination signal associated with the first cDNA, it is expected to trigger expression of the second cDNA (HA-tagged). We refer to this genotype as $wg^{KO}[F\text{-}Wg^{OLLAS}\text{-}F\text{-}Wg^{HA}]$. Neither tag affected protein functionality, as indicated by the fact that homozygous $wg^{KO}[F\text{-}Wg^{OLLAS}\text{-}F\text{-}Wg^{HA}]$ flies (Supplementary Fig. 1 b), as well as homozygous $wg^{KO}[Wg^{HA}]$ flies [6] are fully viable, with a normal wing margin. Since the wing margin is particularly sensitive to reduced Wingless signalling [7], these observations confirm that both $Wingless^{OLLAS}$ and $Wingless^{HA}$ have full signalling activity. Expression of Flp throughout the posterior compartment (under the control of *hedgehog-Gal4*) led to complete conversion from one tag to another (Supplementary Fig. 1 c), showing that the $F\text{-}Wg^{OLLAS}\text{-}F$ cassette is readily excised. To make expression inducible, a *tubulin-Gal80*^{ts} transgene was introduced (Fig. 2 a). At 18°C, $Gal80^{ts}$ is active, preventing Gal4 from triggering Flp expression. Shifting to 29°C inactivates $Gal80^{ts}$, inducing Flp expression and hence causing expression from the *wingless* locus to switch from $Wingless^{OLLAS}$ to $Wingless^{HA}$. The switch occurred with a delay, as expected, and with some cell-to-cell heterogeneity. Nevertheless a clear temporal sequence could be seen. The first signs of HA immunoreactivity in permeabilised discs appeared 2 hours after the temperature shift. At this time, 95% of all HA-positive punctae were found in the apical half (n=55) and the majority of them (87%) overlapped with a Golgi marker (anti-GMAP) (Fig. 2 d). This confirms that Wingless is translated and processed in apically-located secretory compartments. From 3 hrs after the temperature shift, the number of HA-positive, GMAP-negative punctae increased to 58% (n=97), likely corresponding to late secretory vesicles or early endosomes (Fig. 2 e). Beyond this time (e.g. 8 hrs after the

temperature shift), HA immunoreactivity was seen to spread in a basal direction (Fig. 2 i). From about 16 hrs after the temperature shift, HA immunoreactivity was seen along the whole apico-basal axis of every HA-positive cells located within the Wingless expressing domain (12 cells from 3 discs analysed), as is the case for wild type Wingless at the steady state. These cells were flanked by HA signal seemingly associated with non-expressing cells (arrows in Fig. 2 j), perhaps representing Wingless released from the basolateral surface. The above observations confirm that Wingless likely undergoes apical-to-basal transport. A paracellular transepithelial route is highly unlikely since there is no evidence that Wingless could reorganise junctional components. Instead, Wingless could either traffic from an apical Golgi compartment directly to the basolateral surface or travel first to the extracellular apical surface before undergoing apico-basal transcytosis.

If Wingless uses the apical surface as a stopover before being endocytosed and trafficked to the basolateral surface, then acute inhibition of endocytosis should lead to apical accumulation of extracellular Wingless. In flies hemizygous for the *shibire*^{ts} allele, all Dynamin-dependent endocytosis arrests within a few minutes after transfer from the permissive temperature of 18°C to the restrictive temperature of 34°C [8, 9]. The distribution of extracellular Wingless was examined in imaginal discs from *shibire*^{ts}/Y larvae cultured for 15, 30 and 60 minutes at 34°C. Within 15 minutes, Wingless was seen to accumulate at the apical surface and this was followed by depletion from the basolateral surface (Fig 2. k-n and Supplementary Fig. 1 d-g). Note that such depletion is expected if supply to the basolateral surface (e.g. from the apical surface) is cut off while Wingless continues to be lost at the basolateral surface (e.g. through release). The *shibire*^{ts} mutation is completely reversible, a feature that allowed us to track the fate of accumulated apical Wingless upon restoration of Dynamin activity following return to 18°C. After 30 minutes at this temperature, extracellular apical Wingless reverted to its low, steady state level. And within a 90 minute period, basolateral Wingless was replenished to the levels seen before the endocytosis block (Fig. 2 o-r and Supplementary Fig. 1 h-k). These results are consistent with the scenario that, in the wild type, Wingless first reaches the apical surface before progressing to the basolateral surface. We suggest that it is from there that Wingless can reach adjoining cells. Further Wingless spread, which has been shown to take place [10], even if it is not absolutely essential [11], is likely to be initiated from the basolateral surface too.

What membrane-associated proteins and trafficking components could be involved in Wingless transcytosis? Glypicans have been shown to undergo transcytosis [12] and it has been suggested from the results of overexpression experiments that the glypican Dally-like (Dlp) could ferry Wingless across the epithelium [13]. To test the requirement of glypicans we removed Dlp as well as Dally, the only other glypican encoded by the *Drosophila* genome, in clonal patches. This caused a mild reduction in the level of extracellular Wingless in receiving cells, as expected from the suggested contribution of these glypicans to the spread of Wingless at the basolateral surface [14]. However, we found no evidence that glypicans also contribute to apical-to-basolateral transport since extracellular Wingless did not accumulate at the apical surface of Wingless-secreting *dally dlp* double mutant cells, while still being detectable at the basolateral surface (Supplementary Fig. 2). Another membrane-associated protein that could conceivably contribute to Wingless transcytosis is the multi-pass transmembrane protein encoded by *wntless/evenness interrupted/sprinter*, here referred to as

Evi [15-17]. Evi and its mammalian homologs are known to interact and traffic with Wingless/Wnts [18, 19] and AP-2 dependent Evi recycling has been suggested to contribute to basolateral secretion of Wnt3A in MDCK cells [20]. However the roles of AP-2 and Evi in transcytosis are hard to test because of AP-2's pleiotropic roles and Evi's requirement for Wingless progression from the ER/Golgi to the plasma membrane [15, 21].

Besides requiring a membrane-associated escort, Wingless transcytosis is likely to involve trafficking regulators, for example to ensure appropriate sorting out of early endosomes. From RNAi-based analysis of various candidates, we found that knocking down *godzilla*, which encodes a PA-TM-RING E3 ubiquitin ligase that regulates recycling endosome trafficking [22], led to loss of wing margin (Fig. 3 a-b), a structure that requires Wingless signalling at the third instar [7]. Accordingly, *godzilla* knockdown (confirmed by immunostaining; Supplementary Fig. 3 a, b) led to a strong reduction in the expression of *senseless* (Fig. 3 c, d), a target of Wingless signalling in late wing imaginal discs [23]. Note that expression of a *wingless-lacZ* enhancer trap was largely unaffected in this context (Supplementary Fig. 3 c), indicating that Notch signalling, which is required for *wingless* transcription at the prospective margin [24], is relatively unaffected by *godzilla* knockdown. However, upon *godzilla* knockdown, the Wingless protein distribution was noticeably restricted, as if confined to the expression domain (Fig. 3 c). Moreover, *godzilla* knockdown caused accumulation of intracellular Wingless in Wingless-expressing cells, particularly in the apical region (Fig. 3 d). To confirm the specificity of this phenotype, we generated homozygous $godzilla^{\Delta 2}$ clones. Unfortunately, large clones could not be recovered, perhaps because they are outcompeted. However, intracellular Wingless was seen to accumulate in the small clones that were generated (Fig. 3 e, f). These observations are consistent with the notion that Godzilla normally helps Wingless to exit early apical endosomes. Previous work has shown that Godzilla regulates endocytic trafficking by ubiquitylating VAMP3, a SNARE protein also known as Synaptobrevin (Syb) in *Drosophila* [22]. We therefore asked whether the role of Godzilla in Wingless trafficking could be mediated by Syb. Induction of *syb* mutant clones (unmarked) caused wing margin defects and *syb* knockdown throughout the posterior compartment led to loss of Senseless expression, suggesting a role for Syb in Wingless signalling (Fig. 3 g-h). The *wingless-lacZ* reporter was unaffected by Syb knockdown (Supplementary Fig. 3 d), suggesting that, as with *godzilla* knockdown, *wingless* transcription is maintained under these experimental conditions. Critically, Wingless was seen to accumulate in *syb* mutant clones (Fig. 3 i-j), the same phenotype as that seen in Godzilla defective cells. The above results suggest that Godzilla, and its target Syb, regulate a post-endocytic event that ensures Wingless transcytosis. Accordingly, Wingless and Godzilla are expected to transit through common Rab5-positive endosomes. Indeed, Wingless and Godzilla were found to colocalise in enlarged endosomes induced by expression of YFP-tagged constitutively active Rab5 (Supplementary Fig. 4 a, b). Likewise overexpression of Godzilla caused the formation of enlarged endosomes where Wingless accumulates (Supplementary Fig. 4 c). It is conceivable therefore that Godzilla could meet Wingless in early endosomes and direct it towards an onward transcytotic route.

To test the contribution of Godzilla to Wingless transcytosis, the distribution of extracellular Wingless was assessed following Godzilla knockdown. As shown in Fig. 4 a-c, this led to apical accumulation and basolateral depletion, the same phenotype seen upon acute

inhibition of endocytosis in *shibire*^{ts}/Y imaginal discs. To confirm this observation we designed a dominant negative version of Godzilla (Gzl.LD) by mutating key residues (His255 and His258) in the RING domain (Fig. 4 d) [22]. Expression of this construct led to the same phenotype as that caused by RNAi-mediated knockdown (Fig. 4 e-g). Also consistent with the results of RNAi knockdown, this was accompanied by impaired signalling, as indicated by wing margin defects and loss of Senseless expression (Supplementary Fig. 4 d-e). We suggest therefore that Godzilla could control a switch that directs cargo (e.g. Wingless) from early endosomes into a transcytotic route. Analysing the role of Godzilla in the behaviour of other transcytosed cargoes will be needed to determine whether Godzilla is a general controller of apical-to-basolateral transcytosis, as suggested by requirement of Godzilla for long term cell viability.

Why does Wingless need to undergo transcytosis? The need for trafficking to the basolateral surface could be explained if Wingless was preferentially released and/or mostly signaled there. We therefore devised an independent experimental test of whether Wingless normally signals from the apical or the basolateral surface. This test relies on the fact that the hemolymph (*Drosophila* blood) has only access to the basolateral surface of imaginal discs. Topologically, the apical surface faces the outside of the larva. We used a Gal4 driver active in the fat body and hemocytes (*cg-Gal4*) to flood the hemolymph with Notum, an enzyme that inactivates Wingless in the extracellular space by removal of its palmitoleate moiety [25]. Since sustained systemic expression of Notum was lethal, Gal80^{ts} was used to induce expression for a limited time. Fifteen hours was found to be compatible with larval viability. During this time, Notum accumulated at imaginal discs and, as a result, expression of *senseless* was inhibited, though to varying degrees, likely depending on the extent of Notum expression in the hemolymph (Fig. 5 a, b). We can not exclude the possibility that some Notum could reach the apical surface in this experimental setup. However we think it is unlikely because wing imaginal discs have been shown to form a tight subapical seal [26]. We conclude therefore that Wingless is unlikely to trigger sufficient signalling (at least to a level that triggers Senseless expression) during its brief transit at the apical surface. Wingless signal transduction is mediated by Arrow (LRP5/6) and the redundant Frizzled and Frizzled2. To further investigate the likely location of signal transduction, we sought to determine the subcellular localisation of Frizzled2. Since no suitable antibodies were available, we modified the *frizzled2* locus such that the product would be tagged with GFP. *In situ* hybridisation has shown that *frizzled2* expression is repressed by Wingless signalling [27]. This was confirmed by the distribution of GFP-Frizzled2, low near the site of Wingless expression and relatively higher further away (Fig. 5 c and Supplementary Fig. 5). Importantly, GFP (hence Frizzled2) was predominantly found at the basal surface (Fig. 5 c). We suggest that this could account, at least in part, for the inability of Wingless to trigger significant signalling activity at the apical surface.

The question remains as to why Wingless needs to transit through the apical surface before reaching the basolateral surface. Several possibilities can be considered. Wingless could somehow require transcytosis in order to become active, perhaps as a result of the pH changes it experiences in endocytic compartments. Indeed acidification in the secretory pathway has been suggested to stimulate Wnt release [18]. Transcytosis could also ensure Wingless release by enabling packaging in exosomes [28] or interaction with a chaperone such

as SWIM [29]. Lastly, Wingless circuitous route out of the cell could be necessary to prevent interaction in the secretory pathway with Notum, which is expected to be coexpressed since it is a target gene [25].

In conclusion, we have shown that Wingless is first presented at the apical surface of wing imaginal disc cells before being transcytosed to the basolateral surface, where it triggers signalling (Fig. 5 d). These results build on earlier evidence that intracellular trafficking modulates Wingless signalling [23]. Transcytosis of Wnt3a has been shown to take place in cultured mammalian cells [20] and Hedgehog, another lipid-modified signalling protein also undergoes transepithelial transcytosis [30], suggesting that it could be a general process. Further work will be needed to determine whether vertebrate Wnt transcytosis occurs *in vivo* and also whether Wg transcytosis takes place in other epithelial tissues of *Drosophila*, such as in the embryonic epidermis. As we have shown, Godzilla, the *Drosophila* homolog of RNF167, a membrane-associated E3 ubiquitin ligase, promotes transcytosis of Wingless and possibly other cargoes. This activity is distinct from that of another membrane-associated ubiquitin ligase RNF43, which triggers the removal of Wnt receptors from the cell surface [31]. It is also distinct from the activity of RNF146, which regulates the degradation of Axin, a component of the β-catenin destruction complex [32]. Thus, RNF43 and RNF146 appear to be specific regulators of Wnt signalling. In contrast, Godzilla and its mammalian counterpart (RNF167) seem to regulate a more pleiotropic process, i.e. transcytosis.

Methods are linked to the online version of the paper at www.nature.com/nature.

METHODS

Immunostaining and microscopy

The following primary antibodies were used: mouse anti-Wingless (1:1000 for standard protocol and 1:300 for extracellular staining; DSHB 4D4), rabbit anti-HA (1:1000, Cell Signalling), rat anti-OLLAS (1:10, Abnova), chicken anti-GFP (1:1000, Abcam), mouse anti-Integrin (1:100, DSHB CF.6G11), mouse anti-Dlp (1:50, DSHB 13G8), guinea pig anti-Senseless (1:1000, gift from H. Bellen), mouse anti-V5 (1:500, Invitrogen), goat anti-GMAP (1:100, gift from S. Munro, MRC-LMB Cambridge) guinea pig anti-Godzilla (1:1500; [22]). Secondary antibodies used were Alexa 488 and Alexa 555 (1:500 for standard protocol and 1:250 for extracellular staining, Molecular Probes). Total and extracellular immunostaining of imaginal discs was performed as previously described [4]. Imaginal discs were mounted in Vectashield with DAPI (Vector Laboratories) and imaged using either a Leica SP5 or LSM710 confocal microscope. Z stacks were generated with 1-1.5 micron intervals. Confocal images were processed with ImageJ (N.I.H), Volocity (PerkinElmer), ZEN2.0 (Zeiss) and Photoshop CS5.1 (Adobe). All XY confocal images show a single confocal section, XZ and YZ projections were created using Volocity. Adult wings were mounted in Euparal (Fisher Scientific) and imaged with a Zeiss Axiophot2 microscope with an Axiocam HRC camera.

Fluorescence *in-situ* Hybridisation (FISH)

L3 larvae were dissected and fixed in 4% Formaldehyde-PBS, washed and quenched with 3% H_2O_2. Discs were then post-fixed in 5% Formaldehyde-PBTween and transferred to hybridisation buffer containing the *wingless* probe overnight. Discs were washed and incubated with anti-DIG (Roche), then biotinylated anti-Sheep (1:200, Jackson laboratories) and the reaction was visualised with a Tyramide signal amplification kit (Perkin Elmer). Discs were mounted in Vectashield and imaged as described above.

Drosophila husbandry and clone induction

Fly stocks were kept at 18°C, 25°C or 29°C on a standard medium consisting of agar, cornmeal and yeast. Crosses were performed at 25°C unless they involved tub-Gal80^{ts}, in which case they were kept at 18°C and moved to 29°C when required (as indicated in the relevant figure). Gal4/UAS-RNAi and Gal4/UAS-Gzl.LD.GFP crosses were conducted at 29°C. To inhibit endocytosis temporarily, *shibire^{ts}* wandering L3 larvae were placed on a grape juice plate in a 34°C water bath for the required time period and fixed afterwards. Endocytosis was restored by returning to 18°C for the relevant time period before fixation. For the production of *dally dlp* double mutant clones (Supplementary Fig. 2), larvae were heat shocked 48hr AEL for 45 min at 37°C and fixed 48hr later, at the wandering L3 stage. To generate *godzilla* mutant clones, *MS1096-Gal4; FRT82B, godzilla$^{\Delta 2}$/TM6* was crossed to *UAS-FLP; FRT82B, Ubi-GFP(S65T)nls, RpS3 /TM6.* To generate *syb^{144}* clones, *FRT42D, Ubi-GFP/CyO* was crossed to *Kr/CyO; hh-Gal4, UAS-FLP/TM3ser*, generating *FRT42D, Ubi-GFP(S65T)nls/CyO; hh-Gal4, UAS-FLP/+*, which were subsequently crossed to *FRT42D, syb^{144}/CyO*.

Genetic modifications

To generate *wg^{KO}[F-Wg^{OLLAS}-F-Wg^{HA}],* DNAs encoding OLLAS and HA tagged Wingless were synthesised (Genewiz) and ligated in front of 1200bp of 3'UTR. The tags were inserted in triplicate, separated by a Gly-Gly spacer, between S[306] and G[307]. Wingless^{OLLAS}-3'UTR and Wingless^{HA}-3'UTR were inserted sequentially in MCS and MCS3 of RIV$^{FRT.MCS.pA.FRT.MCS3.pA}$ [6]. The resulting construct, *RIV-F-Wg^{OLLAS}-F-Wg^{HA}* was inserted into the *attP* site of the *wg^{KO}* [6].

To generate flies allowing conditional expression of dominant negative Godzilla, the *godzilla* cDNA was mutated such that two conserved His of the RING domain (His255 and His258) reported to be involved in the coordination of Zn^{2+} ions would be substituted to Arg. The resulting DNA was ligated to DNA encoding EGFP to generate Godzilla.LD.GFP and transferred between the EcoRI and XhoI sites of pUAST before P-element mediated transformation by BestGene (CA).

To obtain animals expressing a GFP-Frizzled2 fusion protein at endogenous level, the *frizzled2* locus was modified by CRISPR-Cas9 stimulated homologous recombination. DNA encoding GFP followed by a LoxP.Pax-Cherry.LoxP cassette was inserted in the *frizzled2* locus such that, after Cre-mediated excision of the cassette, the endogenous gene product would contain GFP (Green below[1]), the peptide encoded by a single LoxP site (Blue below[1]), and a Gly-Ser linker (Red below[1]), all inserted between A29 and D30 of Frizzled2

(i.e. downstream of signal sequence). The engineered allele was confirmed by sequencing the junction between the DNA sequences encoding GFP and Frizzled2.

A_{29}VSKGEEL---MDELYKITSYNVCYTKLCGSSGSSGSSGSD_{30}

Other Drosophila strains

shibire^{ts1} (A Gift from Cahir O'Kane, Cambridge University)

FRT82B (BL 2035)

FRT82B, Ubi-GFP(S65T)nls, RpS3/TM6sb (BL 5627)

FRT42D (BL 1802)

FRT42D, Ubi-GFP(S65T)nls/CyO (BL 5626)

FRT2A, Ubi-GFP (BL 1626)

UAS-YFP.Rab5.Q88L (BL 9774)

UAS-Dcr2; en2.4-Gal4, UAS-EGFP (BL 25752)

UAS-gzl^{RNAi} (VDRC 109001KK)

UAS-syb^{RNAi} (VDRC 102922KK)

FRT82B, godzilla$^{\Delta 2}$/TM3sb [22]

FRT42D, syb^{144}/CyO [33] (A Gift from Cahir O'Kane, Cambridge University)

FRT2A, dally^{MH32}, dlp^{MH20} [34]

UAS-Notum-V5 [25]

UAS-Gzl.WT.GFP [22]

hedgehog-Gal4 and *hedgehog-Gal4, UAS-FLP/tb* [34]

hedgehog-Gal4, tub-Gal80^{ts}/tb, generated with *tub-Gal80^{ts}* (BL7017)

cg-Gal4 (BL 7011)

Drosophila genotypes listed by figures

Figure 1 a-i: *w^{1118}*

Figure 2 a-j: wg^{KO}[F-Wg^{OLLAS}-F-Wg^{HA}]/UAS-Flp; hedgehog-Gal4, tub-Gal80^{ts}/+

Figure 2 k-r: *shibire^{ts}*

[1]Web version of manuscript only

Figure 3 a-d: *UAS-GzlRNAi^{109001KK}/+; hedgehog-Gal4/UAS-mCD8.GFP*

Figure 3 e, f: *MS1096-Gal4/+; UAS-FLP/+; FRT82B, godzilla^{A2}/ FRT82B, Ubi-GFP(S65T)nls, RpS3*

Figure 3 g: (left; control) *FRT42D/ FRT42D, Ubi-GFP(S65T)nls; hedgehog-Gal4, UAS-FLP/+*, (right; experimental) *FRT42D, syb^{144}/ FRT42D, Ubi-GFP(S65T)nls; hh-Gal4, UAS-FLP/+*

Figure 3 h: *UAS-SybRNAi^{102922KK}/+; hedgehog-Gal4/UAS-mCD8.GFP*

Figure 3 i, j: *FRT42D, syb^{144} /FRT42D, Ubi-GFP(S65T)nls; hedgehog -Gal4, UAS-FLP/+*

Figure 4 a-c: *UAS-Dcr2/+; en2.4-Gal4, UAS-EGFP/UAS-GzlRNAi^{109001KK}*

Figure 4 e-g: *UAS-Gzl.LD.GFP/+; hedgehog-Gal4/+*

Figure 5 a: *UAS-Notum-V5/CyO; tub-Gal80^{ts}/+* @ 29°C for 15 hrs before fixation

Figure 5 b: *cg-Gal4/UAS-Notum-V5; tub-Gal80^{ts}* @ 29°C for 15 hrs before fixation

Figure 5 c: *frizzled2^{GFP-KI}*

Supplementary Figure 1: *w^{1118}*

Supplementary Figure 1 b: *wg^{KO}[F-Wg^{OLLAS}-F-Wg^{HA}]/wg^{CX4}*

Supplementary Figure 1 c: *wg^{KO}[F-Wg^{OLLAS}-F-Wg^{HA}]/+; hedgehog-Gal4, UAS-Flp/+*

Supplementary Figure 1 d-k: *shibire^{ts}*

Supplementary Figure 2: *yw hsflp/+;; FRT2A ubi-GFP/FRT2A dally^{MH32} dlp^{MH20}*

Supplementary Figure 3 a, b: *UAS-GzlRNAi^{109001KK}/+; hedgehog-Gal4/UAS-mCD8.GFP*

Supplementary Figure 3 c: *UAS-GzlRNAi^{109001KK}/CyOwglacZ; hedgehog-Gal4/UAS-mCD8.GFP*

Supplementary Figure 3 d: *UAS-SybRNAi^{102922KK}/CyOwglacZ; hedgehog-Gal4/UAS-mCD8.GFP*

Supplementary Figure 4 a, b: *MS10960-Gal4/+; UAS-YFP.Rab5.Q88L/+*

Supplementary Figure 4 c: *MS10960-Gal4/+; UAS-Gzl.WT.GFP/+*

Supplementary Figure 4 d-e: *UAS-Gzl.LD.GFP/+; hedgehog-Gal4/+*

Supplementary Figure 5: *frizzled2^{GFP-KI} /frizzled2^{GFP-KI}*

Europe PMC Funders Author Manuscripts

Supplementary Material

Refer to Web version on PubMed Central for supplementary material.

Acknowledgements

This work was supported by the MRC (U117584268 to JPV), the European Union (ERC grant WNTEXPORT; 294523 to JPV), the Swedish Cancer Society (15/391 to RHP), the Swedish Children Cancer Foundation (2015-0096 to RHP), the Swedish Research Council (2015-04466 to RHP) and the SSF Programme Grant (RB13-0204 to RHP). We thank the Centre for Cellular Imaging (CCI) at the University of Gothenburg for providing confocal imaging support. We are indebted to Luis-Alberto Baena-Lopez for devising the idea of tag switching, to Cahir O'Kane for providing the *syb*^{144} allele, to Hisashi Nojima for help with generating Fig. 5 c and Supplementary Fig. 5 and Yohanns Bellaiche for discussion. We are also grateful to SWEDBO for organising the conference where our collaboration began.

References

1. Tuma PL, Hubbard AL. Transcytosis: crossing cellular barriers. Physiological reviews. 2003; 83:871–932. [PubMed: 12843411]
2. Wilkie GS, Davis I. Drosophila wingless and pair-rule transcripts localize apically by dynein-mediated transport of RNA particles. Cell. 2001; 105:209–219. [PubMed: 11336671]
3. Simmonds AJ, dosSantos G, Livne-Bar I, Krause HM. Apical localization of wingless transcripts is required for wingless signaling. Cell. 2001; 105:197–207. [PubMed: 11336670]
4. Strigini M, Cohen SM. Wingless gradient formation in the Drosophila wing. Current Biology. 2000; 10:293–300. [PubMed: 10744972]
5. Wu J, Klein TJ, Mlodzik M. Subcellular localization of frizzled receptors, mediated by their cytoplasmic tails, regulates signaling pathway specificity. PLoS biology. 2004; 2:E158. [PubMed: 15252441]
6. Baena-Lopez LA, Alexandre C, Mitchell A, Pasakarnis L, Vincent JP. Accelerated homologous recombination and subsequent genome modification in Drosophila. Development (Cambridge, England). 2013; 140:4818–4825.
7. Couso JP, Bishop SA, Martinez Arias A. The wingless signalling pathway and the patterning of the wing margin in Drosophila. Development (Cambridge, England). 1994; 120:621–636.
8. van der Bliek AM, Meyerowitz EM. Dynamin-like protein encoded by the Drosophila shibire gene associated with vesicular traffic. Nature. 1991; 351:411–414. [PubMed: 1674590]
9. Kicheva A, et al. Kinetics of morphogen gradient formation. Science. 2007; 315:521–525. (New York, NY). [PubMed: 17255514]
10. Zecca M, Basler K, Struhl G. Direct and long-range action of a wingless morphogen gradient. Cell. 1996; 87:833–844. [PubMed: 8945511]
11. Alexandre C, Baena-Lopez A, Vincent J-P. Patterning and growth control by membrane-tethered Wingless. Nature. 2014; 505:180–185. [PubMed: 24390349]
12. Mertens G, Van der Schueren B, van den Berghe H, David G. Heparan sulfate expression in polarized epithelial cells: the apical sorting of glypican (GPI-anchored proteoglycan) is inversely related to its heparan sulfate content. The Journal of cell biology. 1996; 132:487–497. [PubMed: 8636224]
13. Gallet A, Staccini-Lavenant L, Therond PP. Cellular trafficking of the glypican Dally-like is required for full-strength Hedgehog signaling and wingless transcytosis. Developmental cell. 2008; 14:712–725. [PubMed: 18477454]
14. Han C, Yan D, Belenkaya TY, Lin X. Drosophila glypicans Dally and Dally-like shape the extracellular Wingless morphogen gradient in the wing disc. Development (Cambridge, England). 2005; 132:667–679.
15. Bänziger C, et al. Wntless, a conserved membrane protein dedicated to the secretion of Wnt proteins from signaling cells. Cell. 2006; 125:509–522. [PubMed: 16678095]

16. Bartscherer K, Pelte N, Ingelfinger D, Boutros M. Secretion of Wnt ligands requires Evi, a conserved transmembrane protein. Cell. 2006; 125:523–533. [PubMed: 16678096]
17. Goodman RM, et al. Sprinter: a novel transmembrane protein required for Wg secretion and signaling. Development (Cambridge, England). 2006; 133:4901–4911.
18. Coombs GS, et al. WLS-dependent secretion of WNT3A requires Ser209 acylation and vacuolar acidification. Journal of cell science. 2010; 123:3357–3367. [PubMed: 20826466]
19. Herr P, Basler K. Porcupine-mediated lipidation is required for Wnt recognition by Wls. Developmental biology. 2012; 361:392–402. [PubMed: 22108505]
20. Yamamoto H, et al. The apical and basolateral secretion of Wnt11 and Wnt3a in polarized epithelial cells is regulated by different mechanisms. Journal of cell science. 2013; 126:2931–2943. [PubMed: 23613470]
21. Yu J, et al. WLS Retrograde Transport to the Endoplasmic Reticulum during Wnt Secretion. Developmental cell. 2014; 29:277–291. [PubMed: 24768165]
22. Yamazaki Y, et al. Goliath family E3 ligases regulate the recycling endosome pathway via VAMP3 ubiquitylation. The EMBO journal. 2013; 32:524–537. [PubMed: 23353890]
23. Seto ES, Bellen HJ. Internalization is required for proper Wingless signaling in Drosophila melanogaster. The Journal of cell biology. 2006; 173:95–106. [PubMed: 16606693]
24. Rulifson EJ, Blair SS. Notch regulates wingless expression and is not required for reception of the paracrine wingless signal during wing margin neurogenesis in Drosophila. Development (Cambridge, England). 1995; 121:2813–2824.
25. Kakugawa S, et al. Notum deacylates Wnt proteins to suppress signalling activity. Nature. 2015; 519:187–192. [PubMed: 25731175]
26. Oshima K, Fehon RG. Analysis of protein dynamics within the septate junction reveals a highly stable core protein complex that does not include the basolateral polarity protein Discs large. Journal of cell science. 2011; 124:2861–2871. [PubMed: 21807950]
27. Cadigan KM, Fish MP, Rulifson EJ, Nusse R. Wingless repression of Drosophila frizzled 2 expression shapes the Wingless morphogen gradient in the wing. Cell. 1998; 93:767–777. [PubMed: 9630221]
28. Gross JC, Chaudhary V, Bartscherer K, Boutros M. Active Wnt proteins are secreted on exosomes. Nature cell biology. 2012
29. Mulligan KA, Fuerer C, Nusse R. 6 Inaugural Article: Secreted Wingless-interacting molecule (Swim) promotes long-range signaling by maintaining Wingless solubility. Proceedings of the National Academy of Sciences of the United States of America. 2011; 109:370–377. [PubMed: 22203956]
30. Callejo A, et al. Feature Article: From the Cover: Dispatched mediates Hedgehog basolateral release to form the long-range morphogenetic gradient in the Drosophila wing disk epithelium. Proceedings of the National Academy of Sciences. 2011; 108:12591–12598.
31. de Lau W, Peng WC, Gros P, Clevers H. The R-spondin/Lgr5/Rnf43 module: regulator of Wnt signal strength. Genes & Development. 2014; 28:305–316. [PubMed: 24532711]
32. Zhang Y, et al. RNF146 is a poly(ADP-ribose)-directed E3 ligase that regulates axin degradation and Wnt signalling. Nature cell biology. 2011; 13:623–629. [PubMed: 21478859]

Methods References

33. Bhattacharya S, et al. Members of the synaptobrevin/vesicle-associated membrane protein (VAMP) family in Drosophila are functionally interchangeable in vivo for neurotransmitter release and cell viability. Proceedings of the National Academy of Sciences of the United States of America. 2002; 99:13867–13872. [PubMed: 12364587]
34. Franch-Marro X, et al. Glypicans shunt the Wingless signal between local signalling and further transport. Development (Cambridge, England). 2005; 132:659–666.

Europe PMC Funders Author Manuscripts

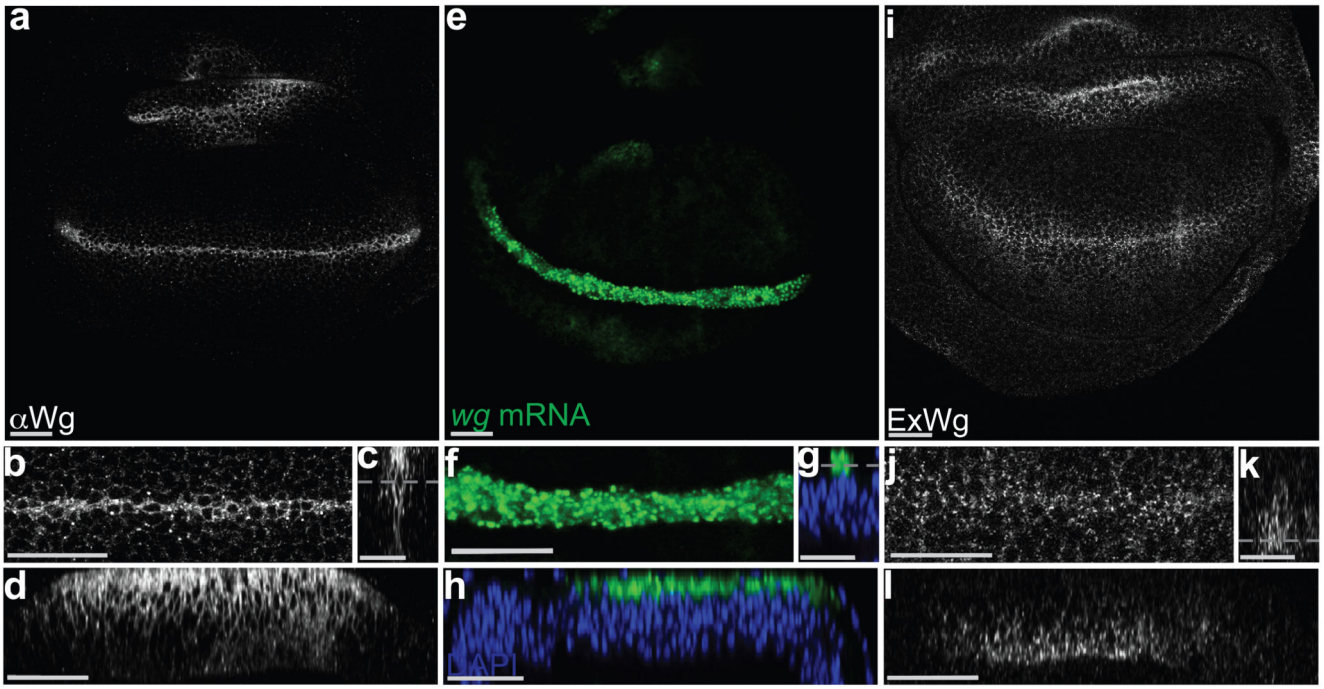

Figure 1. Apical accumulation of intracellular Wingless and basolateral enrichment of extracellular Wingless

a-d, 3rd instar wing imaginal discs stained with anti-Wingless in the presence of detergent. The various panels show the whole pouch (a), a magnified view (b), a cross-section (c) and a longitudinal section (d) of the expression stripe. Note the relative accumulation of Wingless in the apical region. **e-h,** Similar views of an imaginal disc processed for *in situ* hybridisation with a *wingless* probe. Most of the signal is also enriched in the apical region. **i-l,** Similar views of an imaginal disc stained to show extracellular Wingless. Here, the signal is much weaker than in panel a-d (not shown at the same gain). Most of the signal is basolateral. A grey dotted line in panels c, g, and k marks the approximate plane of focus of the images shown in panels a/b, e/f, and i/j respectively. Apical is shown at the top in this and all subsequent figures. Every picture is representative of data from >10 discs from 3 independent experiments. Scale bars represent 24 μm.

Europe PMC Funders Author Manuscripts

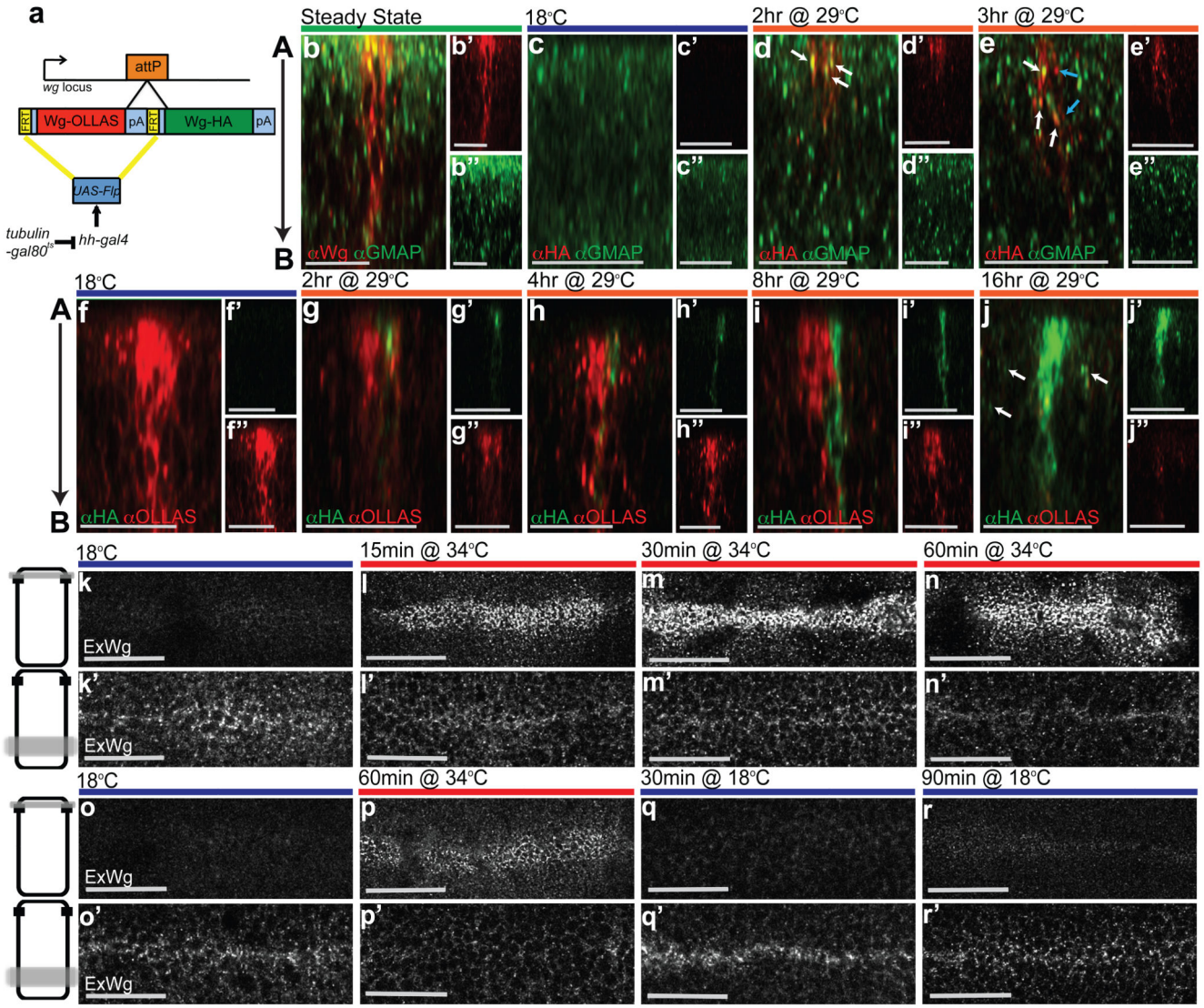

Figure 2. Tracking the progress of Wingless along the apico-basal axis

a, Diagram depicting the tag switching construct inserted at the *wingless* locus. **b,** Steady state distribution of endogenous Wingless relative to the Golgi marker GMAP in a 3rd instar wing imaginal disc. 82% of Wingless-positive punctae are in the apical half (n= 175). **c**, Absence of HA immunoreactivity in an imaginal disc from $wg^{KO}[F\text{-}Wg^{OLLAS}\text{-}F\text{-}Wg^{HA}]$/ *UAS-Flp*; *hedgehog-Gal4 tub-Gal80*^{ts} larva cultured at 18°C. **d,** HA immunoreactivity can be seen 2 hrs after transfer to 29°C and mostly colocalises with GMAP (white arrows). **e,** From 3 hrs onwards, anti-HA is found in both GMAP-negative (blue arrows) as well as GMAP-positive (white arrows) vesicles. **f,** Steady state distribution of Wingless^{OLLAS} in a $Wg^{OLLAS}\text{-}F\text{-}Wg^{HA}$]/*UAS-Flp*; *hedgehog-Gal4 tub-Gal80*^{ts} imaginal disc. Note the absence of Wingless^{HA}. **g, h,** HA immunoreactive vesicles first appear in the apical region 2 hrs the after temperature shift (g), and increase in number during the following 2 hrs (h). **i,** Wingless^{HA} is seen at ever more basolateral positions 8 hrs after transfer to 29°C. **j,** Another 8 hrs later, Wingless^{HA} has completely replaced Wingless^{OLLAS} and HA immunoreactivity

Europe PMC Funders Author Manuscripts

can also be detected in nearby non expressing cells (white arrows). **k,** This and all subsequent panels show hemizygous *shibire*^{ts} wing imaginal discs at 3rd instar. When endocytosis is allowed to proceed normally (18°C), steady state extracellular Wingless is mainly found at the basolateral surface (approximate plane of focus is shown as a grey line across a diagrammatic cell on the left). **l-n,** Preventing Dynamin-dependent endocytosis leads to Wingless accumulation at the apical surface and concomitant depletion from the basolateral surface (15, 30, and 60 min at 34°C). **o,** Steady state extracellular Wingless with normal endocytosis (18°C). **p,** Extracellular Wingless after endocytosis block (60 min at 34°C). **q, r,** Restoration of Dynamin activity by transfer to 18°C for 30 min (q) and 90 min (r). This leads to removal of accumulated apical extracellular Wingless and replenishment of the basolateral pool. Data from panels b-j, i.e. the number of punctae, as provided in the text, were pooled from at least 3 discs per experimental condition. Each time point in panels k-n is representative of >10 discs from 3 independent experiments. For panels o-r, >5 discs from three independent experiments were analysed. Scale bars represent 20 μm in b-j and 24 μm in k-r.

Europe PMC Funders Author Manuscripts

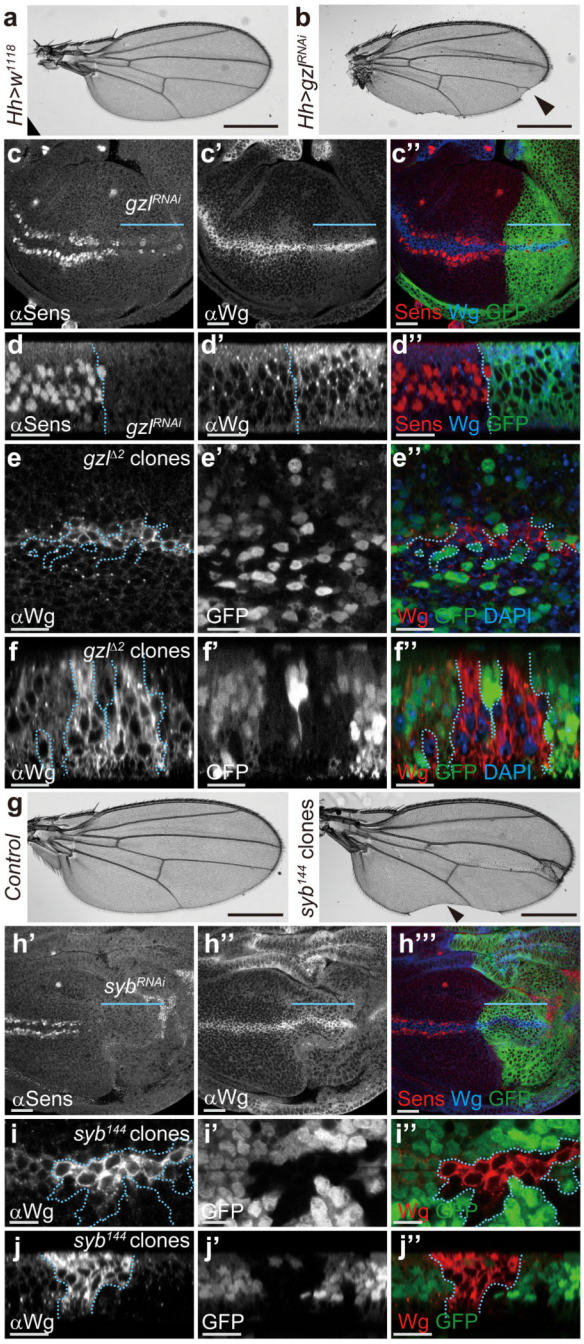

Figure 3. Loss of Godzilla or Synaptobrevin interferes with Wingless signaling and trafficking

a, b, Depletion of *godzilla* by RNAi in the posterior compartment (*hedgehog-Gal4; UAS-gzl*^{RNAi}) results in loss of margin in adult wings (*arrowhead* in b). **c, d,** Expression of the *godzilla* RNAi transgene in the P compartment of 3rd instar imaginal discs, marked by coexpression of GFP in c" and d" and indicated by a blue line in c, c', and c", causes loss of Senseless expression (c, d) and Wingless accumulation (c', d'). The GFP-negative compartment serves as control. Note that residual Senseless remains in the affected territory, in a somewhat variable fashion. Panels c-c" show subapical plane and panels d-d" an optical

transverse section. Pictures are representative of >10 discs. **e, f,** Accumulation of Wingless protein in *godzilla*$^{\Delta 2}$ (*gzl*$^{\Delta 2}$) clones marked by the absence of GFP. Panel e shows a subapical plane and panel f an optical transverse section. **g,** Adult wing bearing unmarked *syb*^{144} mutant clones have notches in the margin (*arrowhead*). 30% of examined discs had a similar phenotype. **h,** Expression of an RNAi transgene against *syb* in the posterior compartment (green in h”’, driven by *hedgehog-Gal4)* leads to loss of Senseless expression. **i, j,** Wingless protein accumulates in Wingless-producing cells that are homozygous for *syb*^{144} (random clones induced in the posterior compartment). Panel i shows a subapical plane and panel j an optical transverse section. All the pictures are representative of >10 samples (wings or discs) from at least three independent experiments. Scale bar = 10 μm except in panels a, b, and g, where it represents 500 μm.

Europe PMC Funders Author Manuscripts

Europe PMC Funders Author Manuscripts

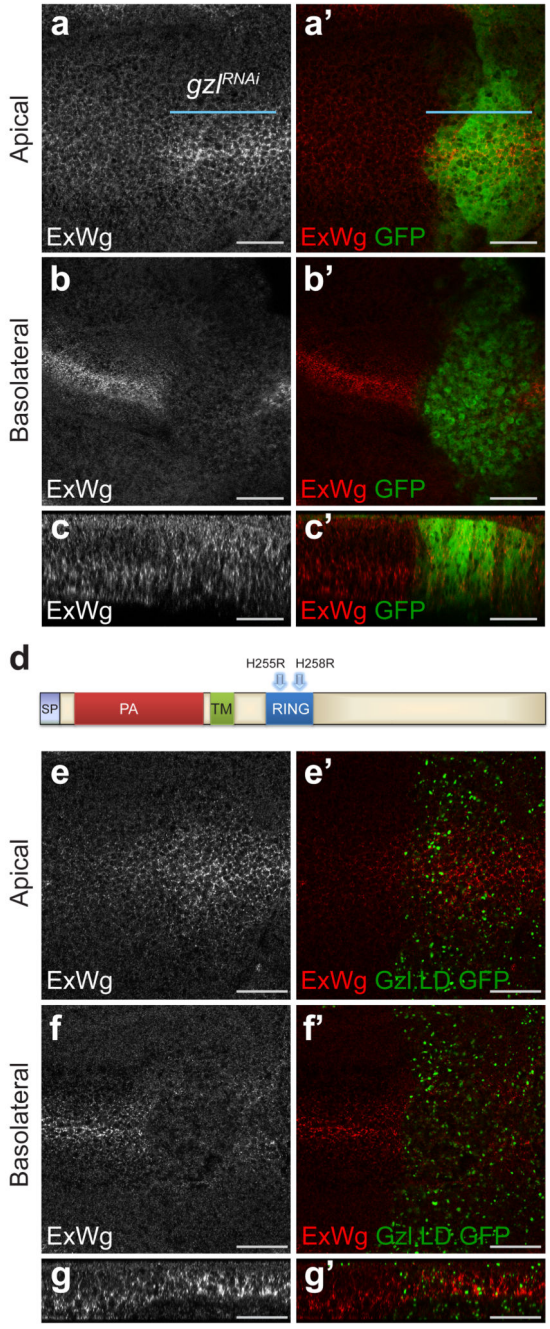

Figure 4. *godzilla* knockdown prevents Wingless transcytosis

a, b, *En face* views of a 3rd instar wing imaginal disc expressing RNAi against *godzilla* (marked by GFP co-expression) in the posterior compartment (with *engrailed-gal4*). Staining for extracellular Wingless shows that *godzilla* RNAi causes Wingless to accumulate at the apical surface (a) and to become depleted from the basolateral surface (b). **c,** The same preparation shown in a transverse optical section. This disc is representative of >10 discs from 2 independent experiments. **d**, Diagram of Godzilla indicating the two conserved residues (His255 and His258) that were mutated to generate a ligase-dead version. **e-g**,

Expression of GFP-tagged ligase-dead Godzilla (Gzl.LD.GFP), phenocopies *godzilla* knockdown: accumulation of extracellular Wingless at the apical surface (e) and depletion at the basolateral surface (f). Panel g shows a transverse optical section. This disc is representative of >10 discs from 3 independent experiments. Scale bars represent 10 μm.

Europe PMC Funders Author Manuscripts

Europe PMC Funders Author Manuscripts

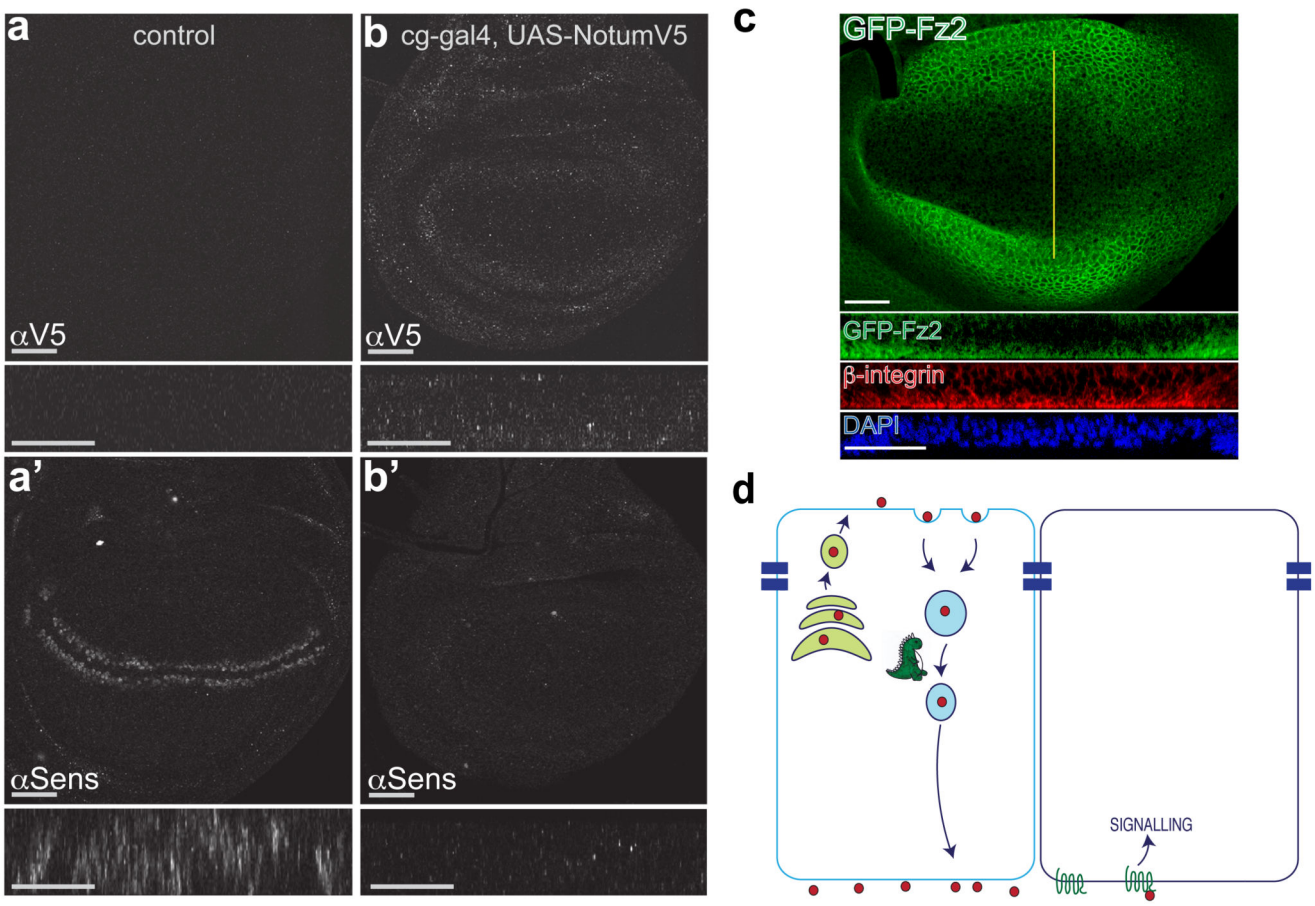

Figure 5. Basolateral Notum originating from the hemolymph inhibits Wingless signalling in wing imaginal disc

a, Control imaginal disc carrying *UAS-Notum*^{V5} and *tubulin-Gal80*^{ts}. No V5 immunoreactivity is detected and expression of Senseless is normal. Main panels show *en face* view while small rectangles show xz reconstruction at the level of the Wingless stripe. **b,** Experimental disc carrying *UAS-Notum*^{V5}, *tubulin-Gal80*^{ts} and *cg-Gal4* (fat body and hemocyte driver). Control and experimental discs were co-cultured first at 18°C to allow growth and survival and then at 29°C for 15 hours to inactivate Gal80^{ts}, hence triggering Notum expression into the hemolymph of experimentals. This led to accumulation of Notum-V5 and loss of Senseless expression. These effects were variable, likely because of suboptimal Notum expression (longer time at 29°C caused larval lethality). The experimental disc shown is representative of 9 discs from 6 larvae. **c,** Distribution of GFP-tagged Frizzled2 (detected with anti-GFP) in 3rd instar imaginal discs. Yellow line indicates position of optical sections shown below (peripodial membrane cropped out for clarity). Most of the staining is found at the basal surface, as shown in the transverse optical section. Note that Frizzled2 is relatively depleted around the source of Wingless, as expected since *frizzled2* is transcriptionally repressed by Wingless signalling[27]. In panels a-c, scale bars represent 24 μm. **d,** Model depicting the role of Godzilla in Wingless transcytosis. Godzilla normally contributes to exit from early endosomes, thus ensuring that Wingless reaches the

basolateral surface where it engages with signalling receptor to trigger target gene expression.

Europe PMC Funders Author Manuscripts